

# Randomly generated spectrum of the solar $f$ -mode

K. Murawski<sup>1</sup> and K. Diethelm<sup>2</sup>

<sup>1</sup> Technical University of Lublin, Department of Environmental Physics, ul. Nadbystrzycka 40, 20-618 Lublin, Poland

<sup>2</sup> Technische Universität Braunschweig, Institut für Angewandte Mathematik, Pockelsstrasse 14, 38106 Braunschweig, Germany

Received 14 January 2000 / Accepted 6 March 2000

**Abstract.** We show that a random flow that depends on space and time generates a mode which is damped and move slower than the coherent  $f$ -mode as well as possesses properties which are consistent with the recent SOHO/MDI data (Antia & Basu 1999).

**Key words:** convection – Sun: atmosphere – Sun: granulation – Sun: oscillations – turbulence

## 1. Introduction

The solar  $f$ -mode is known as a surface gravity wave which, for a high horizontal wavenumber  $k$  and the frequency  $\omega_0$ , satisfies the parabolic dispersion relation  $\omega_0^2 = gk$ , where  $g$  is the surface gravity of the Sun. However, according to observations the  $f$ -mode frequency departs from the frequency given by the above dispersion relation and the line-width grows with  $k$  (Libbrecht et al. 1990; Rhodes et al. 1991; Fernandes et al. 1992; Bachmann et al. 1995; Duvall et al. 1998; Antia & Basu 1999).

A theoretical explanation of the observed properties of the  $f$ -mode was presented by Murawski & Roberts (1993) who showed that the  $f$ -mode reduces its frequency as it spends more time propagating against a space-dependent random flow than with the flow. As a result of that, its effective speed and consequently frequency are reduced. The interaction between the wave and a random flow scatters coherent energy into incoherent energy by exciting random waves and results in attenuation of the  $f$ -mode and consequently in line broadening. The random scattering will also affect the phase of each mode; hence the phase speed is changed.

The purpose of this paper is to display the effect of the random flow, that occurs in the convection zone, on the spectrum of the  $f$ -mode oscillations. In particular, we aim to consider space- and time-dependent random flows that may be associated with granules. We present a dispersion equation which is solved numerically for the three cases: a space-dependent random flow, a time-dependent random flow, and a space- and time-dependent random flow. Numerical results show that the effect of a space-dependent turbulent flow is to reduce frequencies and attenuate

the  $f$ -mode, while a time-dependent random flow increases frequencies and amplifies the  $f$ -mode.

The paper is organized as follows. We start by setting up the problem in Sect. 2, where we present the dispersion relation for the random  $f$ -mode. In the following section, we investigate the influence of the flows on spectrum of the solar  $f$ -mode. We compare this spectrum with the results of recent observations by the SOHO/MDI (Antia & Basu 1999). The Appendix describes the method which is used for the evaluation of the improper integrals arising in this context.

## 2. Random dispersion relation

Using a plane parallel one-dimensional model for the solar equilibrium, we consider the  $f$ -mode that propagates along an interface between two semi-infinite layers of perfect gas that is stratified under gravity  $g = 274 \text{ m/s}^2$ . The upper layer represents the solar corona of zero mass density and the lower layer corresponds to the convection zone. The temperature exhibits a discontinuity at the interface, while the gas pressure is continuous there. It is assumed that the plasma is inviscid and incompressible as well as free of a magnetic field, i. e. the motions are described by incompressible ideal hydrodynamic equations.

We assume that at the equilibrium a weak random flow occurs in the convection zone only and that this flow is both space- and time-dependent. This flow satisfies Gaussian statistic, possesses characteristic spatial  $l_x$  and temporal  $l_t$  scales, and its magnitude is  $\sigma$ . To obtain the random velocity field correction to the parabolic dispersion relation we adopt the assumption of the binary collision approximation in a perturbative method (Howe 1971). This model is described in details by Murawski & Roberts (1993).

The normalized horizontal wavenumber  $K = kl_x$  and the normalized frequency  $\Omega = \omega l_t$  of the  $f$ -mode satisfy the following dispersion relation

$$\begin{aligned}
 K - \frac{l_x}{gl_t^2} \Omega^2 & \\
 &= \frac{4\sigma^2}{\pi^2 g^2 l_t^2} K \Omega \int_{-\infty}^{\infty} \int_{-\infty}^{\infty} \frac{\hat{\Omega} \hat{K} e^{-(\hat{\Omega}-\Omega)^2} e^{-(\hat{K}-K)^2} d\hat{\Omega} d\hat{K}}{\hat{K} - \frac{l_x}{gl_t^2} \hat{\Omega}^2}.
 \end{aligned} \tag{1}$$

From this dispersion relation it follows that the dependence of the cyclic frequency  $\Omega$  on the wavevector  $K$  differs from the

non-turbulent dispersion relation that is given by the left hand side of this equation.

### 3. Numerical results

In this section we consider the numerical solutions of random dispersion relation (1). We have solved this equation numerically using the method which is described in details in the Appendix. See also Damelin & Diethelm (1999).

In the following figures, the frequency difference  $\Delta\nu \equiv \nu - \nu_0$  and the imaginary part of the frequency,  $\text{Im}(\nu)$ , are displayed as functions of the spherical degree  $l$ . The quantity  $\Delta\nu$  is obtained by determining  $\nu = \omega/2\pi$  numerically from dispersion relation (1) and then subtracting the cyclic frequency  $\nu_0 = \omega_0/2\pi$  that pertains in a static convection zone. As a consequence of scattering by turbulent flow, the energy of the  $f$ -mode is partially transferred between the turbulent and coherent fields. This phenomenon is associated with the imaginary part of the frequency,  $\text{Im}(\omega)$ . The SOHO/MDI data (Antia & Basu 1999) is shown by the triangles for comparison purposes.

Fig. 1a presents the frequency difference  $\Delta\nu$  as a function of the angular degree  $l$  for a space-dependent random flow with its magnitude  $\sigma = 1$  km/s and the spatial scale  $l_x = 1000$  km. The space-dependent random flow shifts the  $f$ -mode frequency. This shift is described by the real part of  $\nu$ . Since the crosses correspond both to negative and positive (not shown) values of  $\Delta\nu$  we conclude that the space-dependent random flow produces both an increase and decrease of the frequency of the  $f$ -mode. The modes which correspond to  $\Delta\nu < 0$  are slowed down by the space-dependent random flow. The modes with  $\Delta\nu > 0$  are speeded up by this flow.

There is a mode which exists for the whole range of  $l$ ; this mode is weakly slowed down for  $l < 1700$ . The other modes, which are represented by asterisks and diamonds, possess cut-offs; they exist only for sufficiently high  $l$ . There is also a solitary mode (square) whose presence is currently unclear.

Since the Howe's method (Howe 1971) is a perturbative method which is valid for low  $\Delta\nu$ , the strongly slowed down modes seem to be artifacts. An existence of the modes with cut-offs has to be verified observationally. As it is generally believed that a space-dependent random field only slows down modes, speeded up modes are not physical and they are not displayed in Fig. 1a.

Fig. 1b illustrates the imaginary part of the frequency,  $\text{Im}(\nu)$ , as a function of the angular degree  $l$  for the case of space-dependent random flow with  $\sigma = 1$  km/s and  $l_x = 1000$  km. All modes correspond to  $\text{Im}(\nu) < 0$ . The modes with  $\text{Im}(\nu) < 0$  are damped; their amplitudes decay in time.

Fig. 2a shows  $\Delta\nu$  as a function of  $l$  for the case of time-dependent random flow with its magnitude  $\sigma = 1$  km/s and the temporal scale  $l_t = 60$  s. There exists a mode that for  $l < 3000$  is speeded up and slowed down for higher values of  $l$ . Fig. 2b shows that the time-dependent random flow generates an amplified mode, i.e. with an amplitude that grows in time.

Fig. 3 combines results for the space- and time-dependent random flow. A mode which is slowed down ( $\Delta\nu < 0$ ) is present

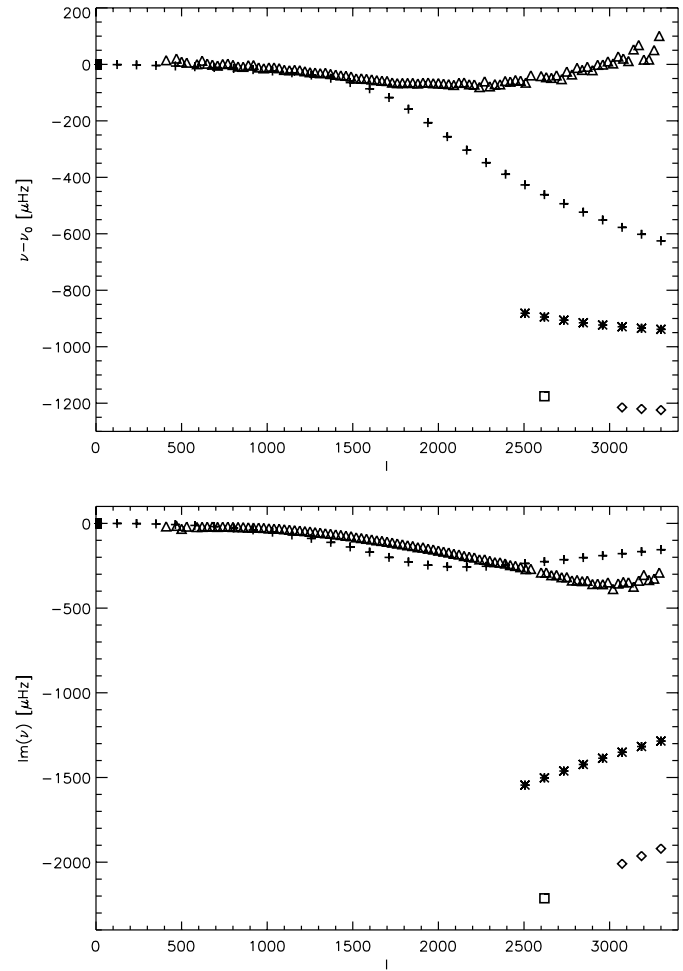


**Fig. 1a and b.** Frequency difference  $\nu - \nu_0$  (top) and imaginary part of the frequency  $\nu$  (bottom) as functions of the angular degree  $l$  for the case of space-dependent random flow with  $\sigma = 1$  km/s and  $l_x = 1000$  km. The crosses represent the data that is obtained from dispersion relation (1). The triangles correspond to the observational SOHO/MDI data (Antia & Basu 1999).

(Fig. 3a). The slowed down mode possesses  $\Delta\nu$  which for  $l < 2200$  is close to the recent SOHO/MDI data (Antia & Basu 1999).

Fig. 3b shows that the damped mode is generated in the case of space- and time-dependent flow. The mode which exists for the entire range of  $l$ , with  $\text{Im}(\nu) < 0$ , possesses frequencies close to the recent SOHO/MDI data (Antia & Basu 1999).

Fig. 4 shows a dependence of the frequency difference and the imaginary part of  $\nu$  on the correlation length  $l_x$  for a space- and time-dependent random flow with its strength  $\sigma = 1$  km/s and the correlation time  $l_t = 600$  s. This value is equal to the granule life-time. The  $f$ -mode is characterized by the angular degree  $l = 1010$ . A perfect fit to the observational data is obtained in the case of  $\Delta\nu$  at  $l \simeq 1.5$  Mm and in the case of  $\text{Im}(\nu)$  at  $l \simeq 1$  Mm. These values of  $l_x$  correspond to granulation. Smaller granules slow down less and damp less the  $f$ -mode.

Fig. 5 illustrates that the  $f$ -mode of  $l = 1010$  is effected by temporal scales too; the flow of high  $l_t$  slows down more and

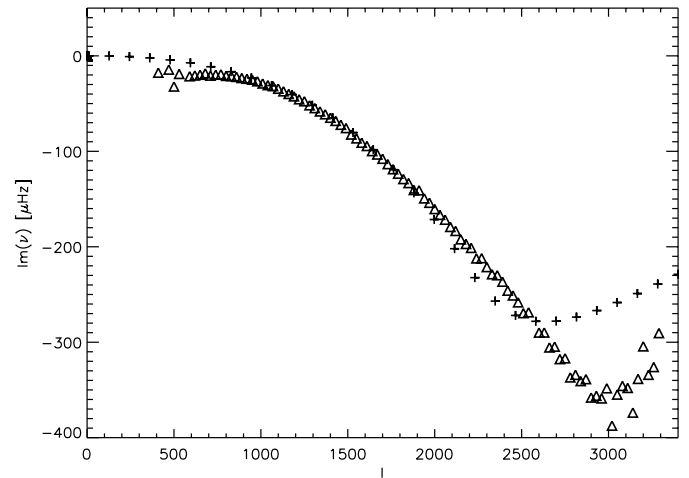
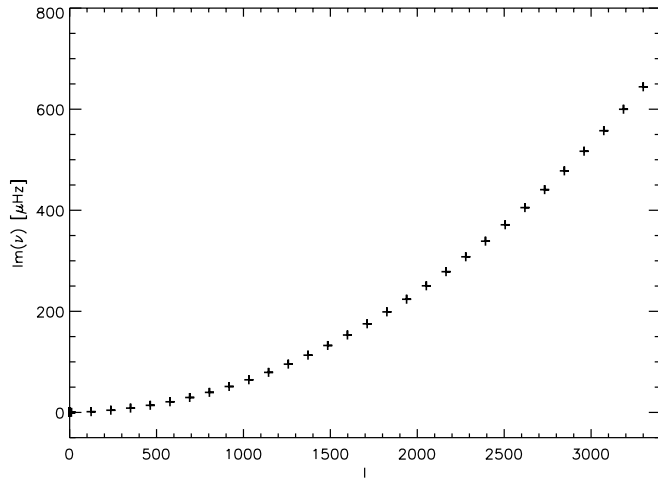
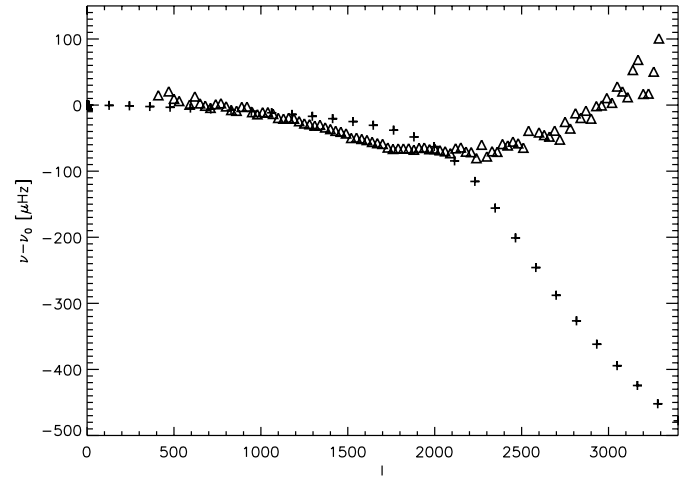
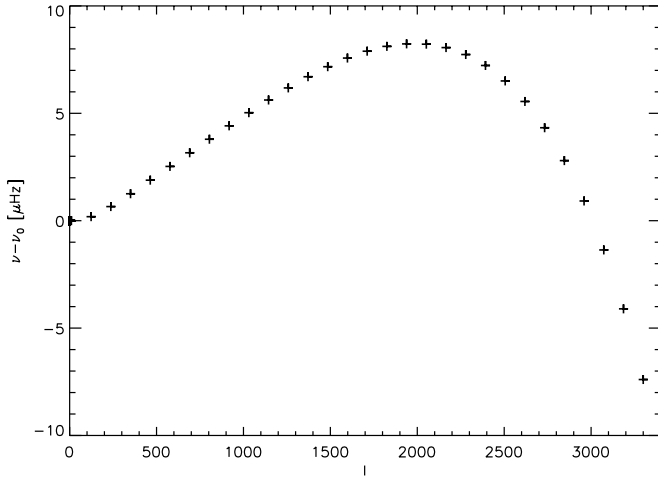


**Fig. 2a and b.** Frequency difference  $\nu - \nu_0$  (top) and imaginary part of the frequency  $\nu$  (bottom) as functions of the angular degree  $l$  for the case of time-dependent random flow with  $\sigma = 1$  km/s and  $l_t = 60$  s. The crosses represent the data obtained from dispersion relation (1).

damps more the  $f$ -mode. A perfect fit to the observational data of  $\Delta\nu$  is obtained at  $l_t \simeq 10$  min. For this value of  $l_t$ ,  $Im(\nu)$  is close to the observational data (Fig. 5b) although the theoretical and observational data do not intersect.

In agreement with former results (e.g., Mędrak & Murawski 2000; Murawski 2000) a stronger random flow reduces more the frequency and damps more the  $f$ -mode (Fig. 6). A perfect fit to the SOHO/MDI data is obtained for  $\sigma \simeq 1$  km/s.

#### 4. Summary

The observed frequencies of the solar  $f$ -mode show deviations from the classical dispersion relation  $\omega^2 = gk$ . We have presented the dispersion relation for the  $f$ -mode in a simple model atmosphere containing a turbulent velocity field. Numerical computations indicate that the effect of the turbulent flow is to shift the frequency and that it can both amplify or damp the  $f$ -mode in dependence whether the flow is time- or space-dependent. The frequency shift is revealed by the real part of  $\omega$ . The imaginary part of this frequency represents the damping or

**Fig. 3a and b.** Frequency difference  $\nu - \nu_0$  (top) and  $Im(\nu)$  (bottom) as functions of the angular degree  $l$  for the case of space- and time-dependent random flow with  $\sigma = 1$  km/s,  $l_x = 1000$  km and  $l_t = 600$  s. The crosses represent the data obtained from dispersion relation (1). The triangles correspond to the observational SOHO/MDI data (Antia & Basu 1999).

amplification of the  $f$ -mode. The  $f$ -mode damping is a result of the generation of turbulent field at the expense of the coherent field. The  $f$ -mode amplification results from an energy transfer from a random flow into the  $f$ -mode.

A random flow generates a mode which is consistent with the properties of the  $f$ -mode obtained from the high-resolution SOHO/MDI data (Antia & Basu 1999).

*Acknowledgements.* This work was financially supported by the grant from the State Committee for Scientific Research Republic of Poland, KBN grant no. 2 PO3D 01717. The authors express their cordial thanks to Prof. Antia for providing the SOHO/MDI data and to Dr. Frank P. Pijpers for his constructive comment. The work of the second author (K. D.) was performed, in part, while he was on leave from the Technical University of Braunschweig, visiting the Mathematics Department at the Justus-Liebig-Universität Gießen (Germany) whose hospitality is gratefully acknowledged. The numerical simulations have been performed at the Department of Complex Systems of the Institute of Physics, UMCS Lublin.

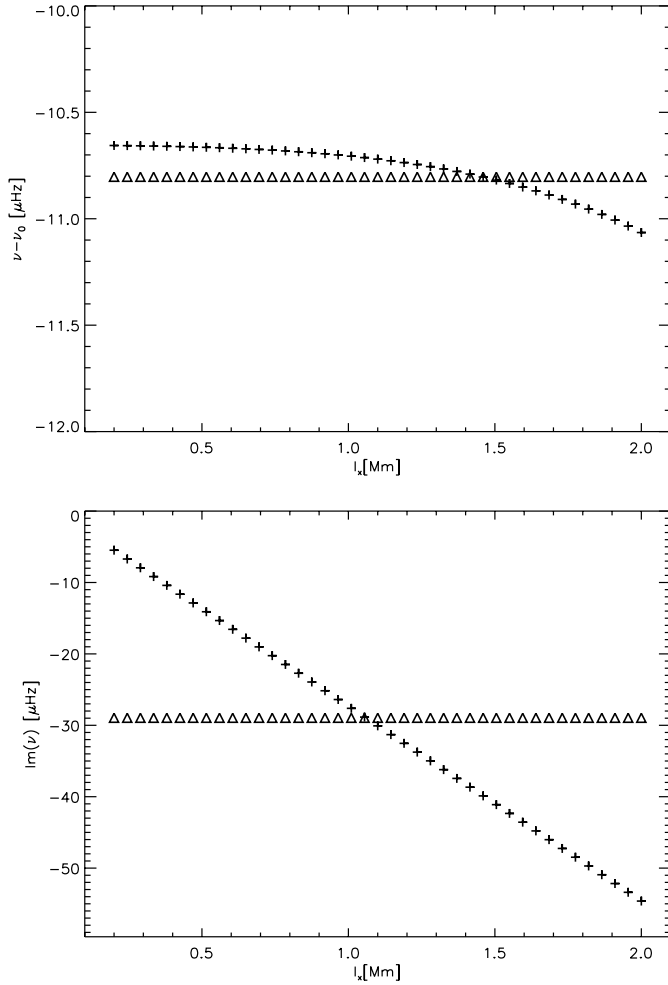


**Fig. 4a and b.** Frequency difference  $\nu - \nu_0$  (top) and imaginary part of the frequency  $\nu$  (bottom) as functions of the correlation length  $l_x$  for the case of space- and time-dependent random flow with  $\sigma = 1$  km/s and  $l_t = 600$  s. The  $f$ -mode possesses the angular degree  $l = 1010$ . The crosses represent the data obtained from dispersion relation (1). The triangles correspond to the observational SOHO/MDI data (Antia & Basu 1999).

#### Appendix: the numerical calculation of improper integrals

In this section we present the numerical scheme that we use for the approximate calculation of the integral

$$\int_{-\infty}^{\infty} \int_{-\infty}^{\infty} f(z_1, z_2) dz_1 dz_2.$$

The integrand functions  $f$  that arise in our application share some typical properties that we shall exploit in order to construct an algorithm that yields a good quality of the approximation without too much computational effort. Specifically, these properties are:

1. For  $|z_j| \rightarrow \infty$ ,  $|f|$  decays as  $\exp(-|z_j|^2)$  ( $j = 1, 2$ );
2. There are certain first-order poles of  $f$  close to, but not on the real axis. The location of these poles is known;

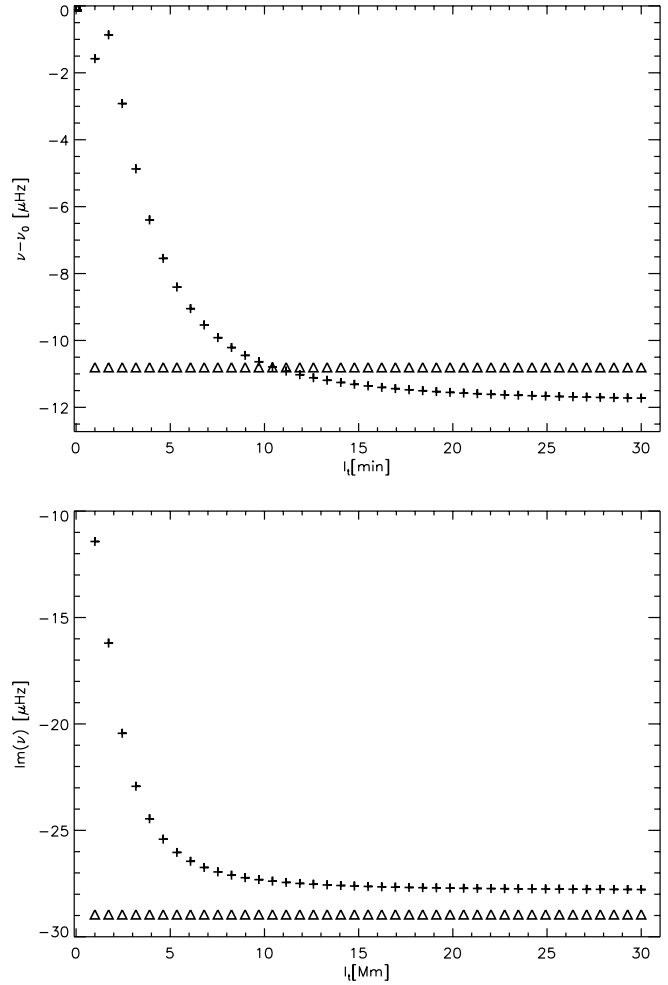


**Fig. 5a and b.** Frequency difference  $\nu - \nu_0$  (top) and imaginary part of the frequency  $\nu$  (bottom) as functions of the correlation time  $l_t$  for the case of space- and time-dependent random flow with  $\sigma = 1$  km/s and  $l_x = 1000$  km. The  $f$ -mode possesses the angular degree  $l = 1010$ . The crosses represent the data obtained from dispersion relation (1). The triangles correspond to the observational SOHO/MDI data (Antia & Basu 1999).

3. The function  $f$  is very smooth (possesses very many, typically infinitely many, continuous derivatives) on the real line.

In view of the structure of the double integral, it seems most natural to use a tensor product type quadrature formula. In other words, we shall begin with a family of quadrature formulas,  $Q_{\alpha, \beta}^{(1)}$ , of the two parameters  $\alpha, \beta \in C$ , defined by

$$Q_{\alpha, \beta}^{(1)}[g] = \sum_{j=1}^n a_j(\alpha, \beta) g(x_j),$$

where  $a_j(\alpha, \beta) \in C$  and  $-\infty < x_1 < x_2 < \dots < x_n < \infty$ , for the one-dimensional integral

$$\int_{-\infty}^{\infty} g(z) dz$$

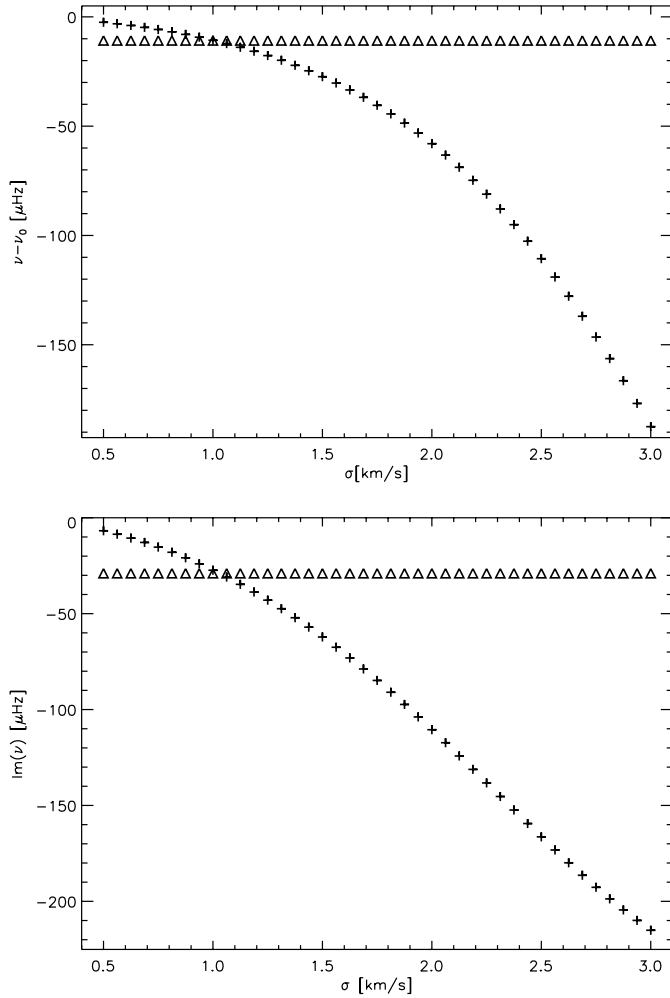


**Fig. 6a and b.** Frequency difference  $\nu - \nu_0$  (top) and imaginary part of the frequency  $\nu$  (bottom) as functions of the variance  $\sigma$  for the case of space- and time-dependent random flow with  $l_x = 1000$  km and  $l_t = 600$  s. The  $f$ -mode possesses the angular degree  $l = 1010$ . The crosses represent the data obtained from dispersion relation (1). The triangles correspond to the observational SOHO/MDI data (Antia & Basu 1999).

and approximate the two-dimensional integral  $\int_{-\infty}^{\infty} \int_{-\infty}^{\infty} h(z_1, z_2) dz_1 dz_2$  by the quadrature formula  $Q_{\alpha, \beta}^{(2)}$  which we define to be the tensor product of two formulas of the  $Q_{\alpha, \beta}^{(1)}$  family,

$$Q_{\alpha_1, \beta_1, \alpha_2, \beta_2}^{(2)}[h] = \sum_{j=1}^n \sum_{k=1}^n a_j(\alpha_1, \beta_1) a_k(\alpha_2, \beta_2) h(x_j, x_k).$$

Now in order to construct the desired efficient quadrature formula, we need to specify the choice of the nodes  $x_1, \dots, x_n$ , and the weights  $a_1(\alpha, \beta), \dots, a_n(\alpha, \beta)$ . This is where we exploit the above mentioned properties of our special integrand function. In view of these properties it seems reasonable to introduce a new function  $\tilde{f}$ , defined in terms of the given integrand  $f$  according to

$$\tilde{f}(z_1, z_2) := \exp(z_1^2 + z_2^2)(z_1 - \alpha_1)(z_1 - \beta_1)$$

$$\times (z_2 - \alpha_2)(z_2 - \beta_2)f(z_1, z_2)$$

where  $\alpha_j$  and  $\beta_j$  are two poles of  $f$  with respect to the  $j$ -th argument. Consequently,

$$\begin{aligned} & \int_{-\infty}^{\infty} \int_{-\infty}^{\infty} f(z_1, z_2) dz_1 dz_2 \\ &= \int_{-\infty}^{\infty} \int_{-\infty}^{\infty} \frac{\exp(-z_1^2) \exp(-z_2^2) \tilde{f}(z_1, z_2) dz_1 dz_2}{(z_1 - \alpha_1)(z_1 - \beta_1)(z_2 - \alpha_2)(z_2 - \beta_2)} \end{aligned}$$

where now  $\tilde{f}(z_1, z_2)$  remains bounded as  $|z_j| \rightarrow \infty$ , and where the points  $\alpha_1$  and  $\beta_1$  or, respectively,  $\alpha_2$  and  $\beta_2$ , are not poles of  $f$ . Then we are left with the problem of finding a suitable one-dimensional quadrature formula  $Q_{\alpha, \beta}^{(1)}$  for the integral

$$\int_{-\infty}^{\infty} \frac{\exp(-z^2)}{(z - \alpha)(z - \beta)} g(z) dz.$$

The exponential factor in this integral gives rise to our choice of the quadrature nodes  $x_1, \dots, x_n$ . According to the results of Damelin & Diethelm (1999), it is advisable in this situation to choose these values as the zeros of the  $n$ -th orthogonal polynomial with respect to the weight function  $\exp(-z^2)$ , i.e. the  $n$ -th Hermite polynomial (Abramowitz & Stegun 1970; Szegő 1975).

In order to achieve a good accuracy, we construct the formula  $Q_{\alpha, \beta}^{(1)}$  to be of interpolatory type, i.e. to be exact whenever the integrand  $\tilde{f}$  is a polynomial of degree not exceeding  $n - 1$ . This is justified in view of the smoothness assumption of  $f$  and hence on  $\tilde{f}$ . According to the classical theory of numerical integration (Davis & Rabinowitz 1984), this gives

$$a_j(\alpha, \beta) = \int_{-\infty}^{\infty} \frac{\exp(-z^2)}{(z - \alpha)(z - \beta)} l_{jn}(z) dz$$

where

$$l_{jn}(z) = \prod_{k=1, k \neq j}^n \frac{x - x_k}{x_j - x_k}$$

is the  $j$ -th Lagrange polynomial associated with our nodes  $x_1, \dots, x_n$ . Hence we find the following final approximation for the integral in question,

$$\begin{aligned} & \int_{-\infty}^{\infty} \int_{-\infty}^{\infty} f(z_1, z_2) dz_1 dz_2 \\ & \approx \sum_{j=1}^n \sum_{k=1}^n a_j(\alpha_1, \beta_1) a_k(\alpha_2, \beta_2) \exp(x_j^2 + x_k^2) \\ & \quad \times (x_j - \alpha_1)(x_j - \beta_1)(x_k - \alpha_2)(x_k - \beta_2) f(x_j, x_k). \end{aligned}$$

Specifically we found satisfactory results with  $n = 9$ . In this case the nodes are given by

$$\begin{aligned} x_1 = -x_9 &= -3.19099320178152760723, \\ x_2 = -x_8 &= -2.26658058453184311180, \\ x_3 = -x_7 &= -1.46855328921666793167, \\ x_4 = -x_6 &= -0.72355101875283757332, \\ x_5 &= 0. \end{aligned}$$

For the efficient calculation of the weights we use the representation

$$\begin{aligned}
 a_j(\alpha, \beta) &= \int_{-\infty}^{\infty} \frac{\exp(-z^2)}{(z-\alpha)(z-\beta)} l_{jn}(z) dz \\
 &= \int_{-\infty}^{\infty} \frac{\exp(-z^2)}{(z-\alpha)(z-\beta)} \left( l_{jn}(z) - \frac{z-\alpha}{\beta-\alpha} l_{jn}(\beta) \right. \\
 &\quad \left. - \frac{z-\beta}{\alpha-\beta} l_{jn}(\alpha) \right) dz \\
 &\quad + \frac{l_{jn}(\beta)}{\beta-\alpha} \int_{-\infty}^{\infty} \frac{\exp(-z^2)}{z-\beta} dz \\
 &\quad + \frac{l_{jn}(\alpha)}{\alpha-\beta} \int_{-\infty}^{\infty} \frac{\exp(-z^2)}{z-\alpha} dz.
 \end{aligned} \tag{2}$$

Here we notice that the integrals in the last line can be expressed as

$$\int_{-\infty}^{\infty} \frac{\exp(-z^2)}{z-t} dz = \pi i \frac{\operatorname{erf}(it) + \operatorname{sgn} \operatorname{Im} t}{\exp(t^2)} =: J(t) \tag{3}$$

where  $\operatorname{erf}$  is the error function and  $i$  is the imaginary unit. The integrand in the remaining integral on the right-hand side of Eq. (2) is a polynomial of degree  $n-3$ , multiplied by  $\exp(-z^2)$ . Hence we can calculate this integral exactly by means of a Gauss-Hermite quadrature formula with at least  $(n/2)$  nodes. It is particularly useful to use the  $n$ -point Gauss-Hermite formula however because then some terms have a particularly simple form. As a result, we obtain (recalling that the function  $J$  was defined in Eq. (3) above)

$$\begin{aligned}
 a_j(\alpha, \beta) &= \frac{1}{\beta-\alpha} \left[ l_{jn}(\beta) J(\beta) - l_{jn}(\alpha) J(\alpha) \right. \\
 &\quad \left. + \sum_{k=1}^n a_k^{\text{GH}} \left( \frac{l_{jn}(\alpha)}{x_k - \alpha} - \frac{l_{jn}(\beta)}{x_k - \beta} \right) \right] \\
 &\quad + \frac{a_j^{\text{GH}}}{(x_j - \alpha)(x_j - \beta)}.
 \end{aligned}$$

Here

$$a_j^{\text{GH}} = \int_{-\infty}^{\infty} l_{jn}(z) \exp(-z^2) dz$$

is the  $j$ -th weight of the  $n$ -point Gauss-Hermite quadrature formula (Davis & Rabinowitz 1984). In our particular case  $n=9$ , we find

$$\begin{aligned}
 a_1^{\text{GH}} &= a_9^{\text{GH}} = 0.00003960697726326438, \\
 a_2^{\text{GH}} &= a_8^{\text{GH}} = 0.00494362427553694722, \\
 a_3^{\text{GH}} &= a_7^{\text{GH}} = 0.08847452739437657329, \\
 a_4^{\text{GH}} &= a_6^{\text{GH}} = 0.43265155900255575020, \\
 a_5^{\text{GH}} &= 0.72023521560605095712.
 \end{aligned}$$

These formulas enable us to calculate the weights  $a_j(\alpha, \beta)$ . In view of the complexity of the final expressions, we do not state them here explicitly.

We note that this construction assumes that there are two poles,  $\alpha_j$  and  $\beta_j$ , with respect to each integration direction. However it is possible and legal to apply the same scheme also in the case when the number of poles is not two.

If only one pole is present or none at all, then we can choose  $\alpha$  and/or  $\beta$  in an arbitrary way, thus introducing (formally) one or two additional poles whose residue is zero (and so, in effect, these poles are not poles after all). In this case no formal modifications to the method are required. There remains, of course, the question of how to choose the location of these artificial poles. In view of the rapid decrease of the exponential factor in the integrand, it is useful to choose this value large in modules, because then the effects of this artifact are damped.

If the integrand has more than two poles (none of which, of course, may be real because otherwise the integral will not exist), then it is advisable to assign  $\alpha$  and  $\beta$  with the values of two of them and ignore the others. One should in this case take into account those two poles that have the most significant effect on the calculations. Typically the presence of the exponential factor will mean that poles with large modules will have little effect. Therefore one should take those poles into account explicitly that have the smallest modules. Alternatively, it is also possible to use those poles that are closest to the interval of integration, i.e. the real axis. However, if there are two poles  $z$  and  $\hat{z}$ , respectively, where  $|\operatorname{Im} z|$  is very small and  $|\operatorname{Re} z|$  is very large, whereas  $|\operatorname{Re} \hat{z}|$  is rather small and  $|\operatorname{Im} \hat{z}|$  is not much larger than  $|\operatorname{Im} z|$ , it is likely that the contribution of  $\hat{z}$  is more significant than the contribution of  $z$  (in view of the magnitudes of  $|z|$  and  $|\hat{z}|$ ), and therefore one preferably ought to use  $\hat{z}$  explicitly.

## References

- Abramowitz M., Stegun I.A., 1970, Handbook of Mathematical Functions. Dover Publ., New York
- Antia H.M., Basu S., 1999, ApJ 519, 400
- Bachmann K.T., Duvall Jr. T.J., Harvey J. W., Hill F., 1995, ApJ 443, 837
- Damelin S.B., Diethelm K., 1999, Numer. Math. 83, 87
- Davis P.J., Rabinowitz P., 1984, Methods of Numerical Integration. 2nd ed., Academic Press, Orlando
- Duvall Jr. T.J., Kosovitshev A., Murawski K., 1998, ApJ 505, L55
- Fernandes D.N., Scherrer P.H., Tarbell T.D., Title A.M., 1992, ApJ 392, 736
- Howe M.S., 1971, J. Fluid Mech. 45, 785
- Libbrecht K.G., Woodard M.F., Kaufman J.M., 1990, ApJS 74, 1129
- Mędrek M., Murawski K., 2000, ApJ 529, 548
- Murawski K., 2000, ApJ, in press
- Murawski K., Roberts B., 1993, A&A 272, 595
- Rhodes E.J., Cacciani A., Korzenik S.G., 1991, Adv. Space Res. 11, (4)17
- Szegő G., 1975, Orthogonal Polynomials. 4th ed., Amer. Math. Soc., Providence